

Tsunami propagation of the 2004 Sumatra earthquake and the fractal analysis of the aftershock activity

V. P. Dimri* & Kirti Srivastava

National Geophysical Research Institute, Hyderabad 500007, India

*[E-mail: director@ngri.res.in]

Received 28 March 2007; revised 18 April 2007

The 26 December 2004, earthquake of magnitude $M_w \sim 9.3$ had generated large tsunami waves that traveled large distances lying along the rim of the Indian Ocean, Bay of Bengal and Arabian Sea and as far as the west coast of Americas causing large scale devastation. The seismicity pattern of the fault zone has been modeled by several authors, and it is seen that the fault rupture can be divided into three segments. The aftershock sequences have been analyzed, using the fractal approach, for three segments independently. The first segment of 500 km long is the zone of the fastest rupture and has the largest fractal dimension of about 2.10 implying that the fault rupture is two dimensional. This region has a lower b value indicative of high stress regime. In this paper the fastest rupture zone has been considered for the generation and propagation of the tsunami waves. The tsunami wave propagation has been modeled using the nonlinear form of long wave equations. The governing equations are expressed as the partial differential equations which have been solved numerically using the finite differences and the tsunami wave heights have been computed at two Gauge locations i.e at Chennai and Visakhapatnam. The wave heights at Chennai and Visakhapatnam have been compared with the tidal data observed at two of these locations. Results show that the arrival times and the magnitude of the wave heights are seen to be in agreement.

[Key words:Tsunami, fractals, gauges, seismicity, Sumatra, earthquake, aftershock activity]

Introduction

The Earthquake of Dec 26, 2004, triggered giant tsunami which propagated throughout the Indian Ocean, (Fig. 1) was the most destructive tsunami experienced. There are several questions which are being addressed and looked into by the scientific community as this event has drastically changed the understanding of the hazard associated by the Tsunamis. Understanding and quantifying all different aspects of this event needs to be documented. The earthquake occurred in a tectonically active region where the Indian plate is subducting beneath the Burmese plate in the Sunda trench. Detailed studies on the rupture process of this earthquake has been reported^{1,2}. The aftershock activity of this earthquake is still continuing till date, probably due the structural readjustments.

The impact of the tsunami was more visible towards Bay of Bengal and Arabian Sea rather than at higher latitude's mainly because the earthquake

occurred at a point that was land locked, more or less from three sides. In the Indian Ocean the tsunami wave propagation was controlled significantly due to reflections. For instance, the Kerala coast line (SE coast of India) was affected by reflections from the

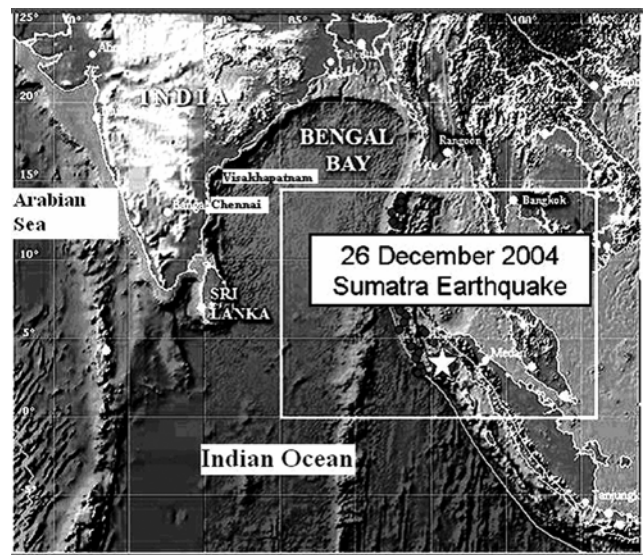


Fig. 1—Regional tectonics of the Sumatra and adjoining areas along with Epicenter of the main shock

*Corresponding author
Phone: 23434600
Fax: 23434651

Lakshadweep Islands. The sustained high water level in the Andaman and Nicobar Islands could be also due to the reflection of direct tsunami waves and trapping of wave energy. They traveled and arrived in North of Sumatra within half an hour after the earthquake and a few hours later they reached Thailand, Sri Lanka, India and Maldives and after about ten hours the tsunami reached the east coast of Africa.

Recently a publication on the 2004 Tsunami from an Indian perspective³ discusses several aspects of the effect of Tsunami on the East and West coasts of India. Dimri & Seivastava⁴ have made a review on modeling techniques of tsunami propagation. The aftershock activity has been analyzed by Ramana *et al.*⁵ for the spatial variation of the b values which is generally dependent on stress regime, material heterogeneity and temperature. In this paper the fractal dimension of the aftershock activity (Fig. 2) has been analyzed and the Tsunami propagation of the 2004 event has been modeled and the wave heights at Chennai (Madras) and Visakhapatnam have been computed.

Materials and Methods

Frequency-magnitude relation of earthquakes—

The frequency-magnitude relation of earthquakes is characterized by the Gutenberg–Richter⁶ power law and which is expressed as

$$\log N = a - b * M \quad \dots (1)$$

where *N* is the cumulative number of earthquakes with magnitude equal to or larger than *M* and *a* and *b* are constants for a given region that may vary in space and time. The constant *b*, is the slope of the log-linear relation and is known as b-value^{7,8}. Often, instead of using the magnitude *M*, the log of seismic moment or the log of energy of the seismic event is used.

The Gutenberg–Richter power law⁶ relation holds good for aftershock sequences too⁹. Depending on the tectonic setting, the stress and the magnitude ranges the b-value generally varies from 0.5 to 1.5. It is observed that for seismically active regions the value is close to 1. Further, it may be noted that b-value can be attributed to the stress distribution after the main shock. The lower b-value indicates higher shear stress and higher b-value is for occurrence of slip¹⁰.

The b-value of any region can be computed using methods like linear least squares regression or by the

Maximum Likelihood Method (MLM). The most robust and widely accepted method is the MLM where the b value is calculated using the formulae¹¹.

$$b = \frac{\log_{10} e}{\bar{M} - M_{\min}} = \frac{0.4343}{\bar{M} - M_{\min}} \quad \dots (2)$$

where \bar{M} is the average of magnitude and M_{\min} is the minimum value of the magnitude for a given data set.

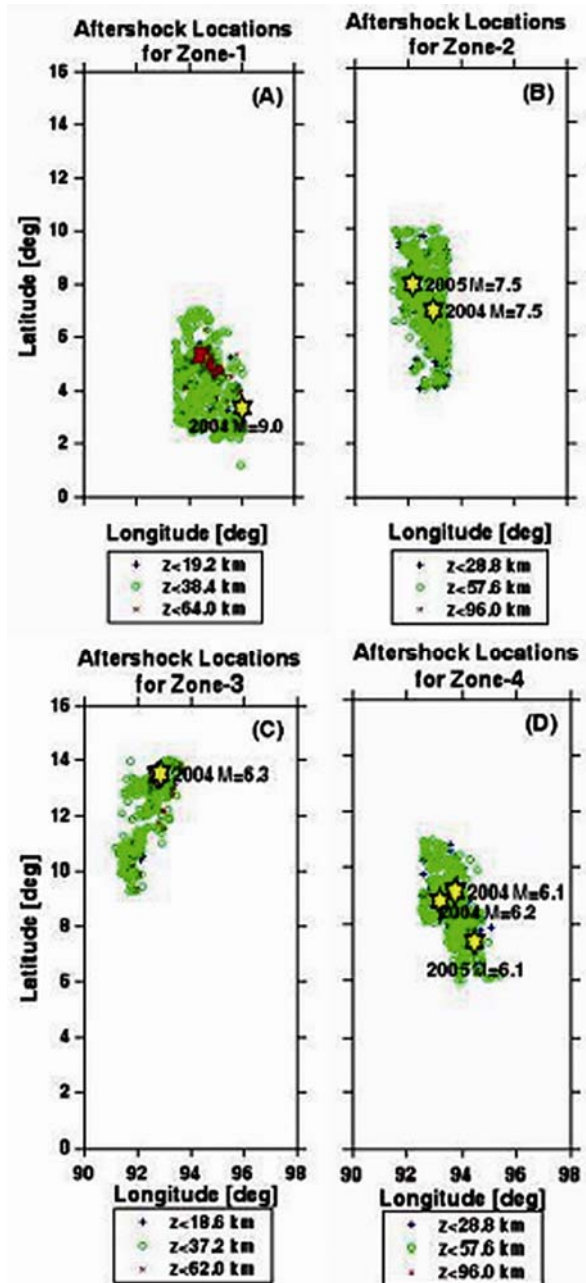


Fig. 2—Seismicity of Sumatra earthquake (A) Zone – 1 (B) Zone – 2 (C) Zone – 3 and (D) Zone – 4

The b value has also been related to the fractal dimension as

$$b = c * \frac{D}{3} \quad \dots (3)$$

where D is the fractal dimension and c is a constant determined from the slope of the log moment versus the magnitude relationship^{12,13}. The value of c is normally taken to be 1.5 but in some cases such as in case of crystalline rocks the value is close to 3.

Mathematical modeling of tsunami waves— Tsunamis are long waves which are mainly generated by the movement of sea bottom due to earthquakes. The vertical acceleration of water particles are negligible compared to the gravitational acceleration except for an oceanic propagation of tsunamis. Thus the vertical motion of water particles has no effect on the pressure distribution.

Neglecting the vertical acceleration the equations of mass conservation and momentum in the three dimension can be expressed as¹⁴:

$$\begin{aligned} \frac{\partial \eta}{\partial t} + \frac{\partial u}{\partial x} + \frac{\partial v}{\partial y} + \frac{\partial w}{\partial z} &= 0 \\ \frac{\partial u}{\partial t} + u \frac{\partial u}{\partial x} + v \frac{\partial u}{\partial y} + w \frac{\partial u}{\partial z} + \frac{1}{\rho} \frac{\partial p}{\partial x} \\ &+ \frac{1}{\rho} \left(\frac{\partial \tau_{xx}}{\partial x} + \frac{\partial \tau_{xy}}{\partial y} + \frac{\partial \tau_{xz}}{\partial z} \right) = 0 \\ \frac{\partial v}{\partial t} + u \frac{\partial v}{\partial x} + v \frac{\partial v}{\partial y} + w \frac{\partial v}{\partial z} + \frac{1}{\rho} \frac{\partial p}{\partial y} \\ &+ \frac{1}{\rho} \left(\frac{\partial \tau_{xy}}{\partial x} + \frac{\partial \tau_{yy}}{\partial y} + \frac{\partial \tau_{yz}}{\partial z} \right) = 0 \\ g + \frac{1}{\rho} \frac{\partial \rho}{\partial z} &= 0 \quad \dots (4) \end{aligned}$$

where x and y are horizontal axes, z the vertical axis, t time, h the still water depth, η the vertical displacement of water surface above the still water surface, u , v and w are water particle velocities in the x , y and z directions, g the gravitational acceleration, and τ_{ij} the normal or tangential shear stress in the i direction on the j normal plane. Equation of momentum in the z -direction with the dynamic conditions at a surface that $p=0$ yields the hydrostatic pressure as $p = \rho g (\eta - z)$.

The dynamic and kinetic conditions at surface and bottom are given as follows:

$$p = 0 \quad \text{at } z = \eta \quad \dots (5)$$

$$w = \frac{\partial \eta}{\partial t} + u \frac{\partial \eta}{\partial x} + v \frac{\partial \eta}{\partial y} \quad \text{at } z = \eta \quad \dots (6)$$

$$w = -u \frac{\partial h}{\partial x} - v \frac{\partial h}{\partial y} \quad \text{at } z = -h \quad \dots (7)$$

Integrate Eq. (4) from the bottom to the surface by Leibnitz rule and applying the dynamic and kinetic conditions we obtain the shallow water equations. For example, the first term of the momentum equation in the x -direction is rewritten as follows:

$$\int_{-h}^{\eta} \frac{\partial u}{\partial t} dz = \frac{\partial}{\partial t} \int_{-h}^{\eta} u dz - u \frac{\partial \eta}{\partial t} \Big|_{z=\eta} + u \frac{\partial(-h)}{\partial t} \Big|_{z=-h}$$

The two dimensional equations obtained are

$$\begin{aligned} \frac{\partial \eta}{\partial t} + \frac{\partial M}{\partial x} + \frac{\partial N}{\partial y} &= 0 \\ \frac{\partial M}{\partial t} + \frac{\partial}{\partial x} \left(\frac{M^2}{D} \right) + \frac{\partial}{\partial y} \left(\frac{MN}{D} \right) + gD \frac{\partial \eta}{\partial x} + \frac{\tau_x}{\rho} \\ &= A \left(\frac{\partial^2 M}{\partial x^2} + \frac{\partial^2 M}{\partial y^2} \right) \\ \frac{\partial N}{\partial t} + \frac{\partial}{\partial x} \left(\frac{MN}{D} \right) + \frac{\partial}{\partial y} \left(\frac{N^2}{D} \right) + gD \frac{\partial \eta}{\partial y} + \frac{\tau_y}{\rho} \\ &= A \left(\frac{\partial^2 N}{\partial x^2} + \frac{\partial^2 N}{\partial y^2} \right) \quad \dots (8) \end{aligned}$$

where D is the total water depth given by $h + \eta$, τ_x and τ_y , the bottom frictions in the x - and y - directions, A the horizontal eddy viscosity which is assumed to be constant in space, the shear stress on a surface wave is neglected. M and N are the discharge fluxes in the x - and y -directions which are

$$\begin{aligned} M &= \int_{-h}^{\eta} u dz = u(h + \eta) = uD \\ N &= \int_{-h}^{\eta} v dz = v(h + \eta) = vD \quad \dots (9) \end{aligned}$$

The bottom friction is generally expressed as follows

$$\frac{\tau_x}{\rho} = \frac{1}{2g} \frac{f}{D^2} M \sqrt{M^2 + N^2}$$

$$\frac{\tau_y}{\rho} = \frac{1}{2g} \frac{f}{D^2} N \sqrt{M^2 + N^2} \quad \dots (10)$$

where f is the friction coefficient. The friction coefficient f and Manning's roughness n are related by

$$n = \sqrt{\frac{fD^{1/3}}{2g}} \quad \dots (11)$$

f becomes rather large when the total depth D is small as n remains almost a constant. The bottom friction terms are then expressed by

$$\frac{\tau_x}{\rho} = \frac{fn^2}{D^{7/3}} M \sqrt{M^2 + N^2}$$

$$\frac{\tau_y}{\rho} = \frac{fn^2}{D^{7/3}} N \sqrt{M^2 + N^2} \quad \dots (12)$$

Using the above equations, the fundamental equations are expressed as follows

$$\frac{\partial \eta}{\partial t} + \frac{\partial M}{\partial x} + \frac{\partial N}{\partial y} = 0$$

$$\frac{\partial M}{\partial t} + \frac{\partial}{\partial x} \left(\frac{M^2}{D} \right) + \frac{\partial}{\partial y} \left(\frac{MN}{D} \right) + gD \frac{\partial \eta}{\partial x} + \frac{gn^2}{D^{7/3}} M \sqrt{M^2 + N^2} = 0$$

$$\frac{\partial N}{\partial t} + \frac{\partial}{\partial x} \left(\frac{MN}{D} \right) + \frac{\partial}{\partial y} \left(\frac{N^2}{D} \right) + gD \frac{\partial \eta}{\partial y} + \frac{gn^2}{D^{7/3}} N \sqrt{M^2 + N^2} = 0 \quad \dots (13)$$

These equations were used to study the propagation of tsunami waves. To model the Tsunami wave, the code is developed based on finite difference technique, adopting the Leap-Frog scheme^{15,16}.

After the Great Sumatra earthquake there has been intense seismic activity which is continuing till date. Considering the magnitude >4.0, the sequence of about 3000 aftershocks is used for analysis. The earthquake hypocentral parameters have been obtained from the NEIC data base¹⁷ for a period of one year since the occurrence of the main event.

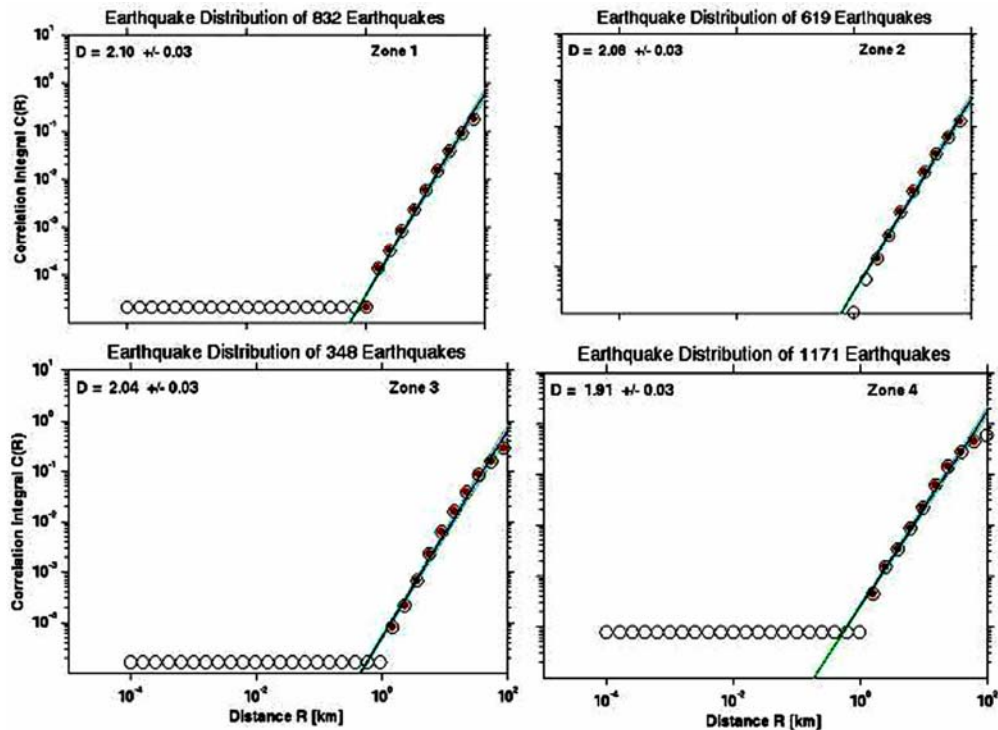


Fig. 3—Fractal analysis of the fault zones

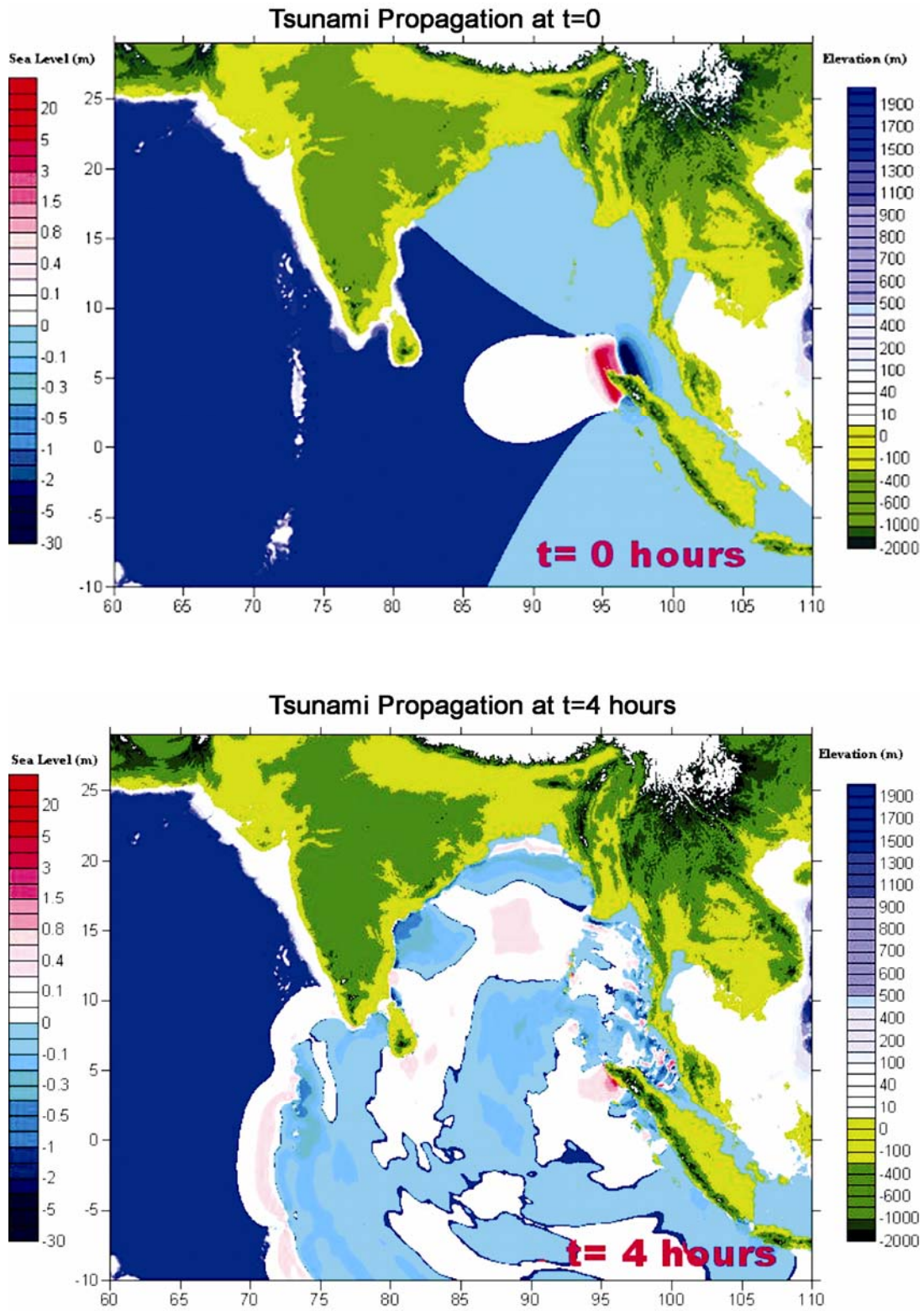


Fig. 4—Tsunami propagation at different times

Figure 1 shows the regional tectonics of the Sumatra region along with the epicenter of the 26 Dec 2004 main shock. Several researchers have studied and analyzed the seismic activity as there was a burst of seismicity in the region after the main shock. The total fault rupture of the main shock in this region was about 1300 km long. According to Ramana *et al.*⁵ a) total fault zone is segmented into four zones i.e., three rupture zones (zone-1, Zone-2, zone-3) and a back arc seismicity (zone-4) (Fig. 2), b). the respective b values of corresponding zones are 0.946, 0.963, 0.972, and 1.21 and c). indicated that the rupture processes has no significant bearing on the frequency-magnitude relationship.

Results

In order to understand the dynamics of the region in detail the fractal analysis is carried out in the present study using the ZMAP Software package¹⁸ the fractal dimension is obtained for all the zones. It is observed that zone 1 has maximum fractal dimension of about 2.10, Zone -2 it is 2.08, Zone-3 it is 2.04 whereas for the back arc seismicity region it is seen to be lower i.e 1.91 (Fig. 3).

The Tsunami waves were modeled using the Tsunami N2 formulation¹⁴. The source parameters for the 2004 Sumatra earthquake¹⁹⁻²¹ were strike angle = 340°, fault length = 500 km, width of the fault = 190 km, focal depth = 25 km, dip angle = 8°, slip angle = 110°, displacement= 20 m. For these parameters the tsunami propagation is carried out. Two gauge locations are considered i.e one at Chennai and the other at Visakhapatnam. Figure 4 shows the tsunami propagation at two different times i.e at the origin and after 4 hours. Figure 5 shows the wave heights at Cheenai and Visakhapatnam. It is noticed that at Chennai the wave height at the gauge is around 85 cm and the wave reached after 2 and half hour. It is seen to be in agreement with the tidal data that has been observed at this location²². Also at Visakhapatnam the tsunami reached after almost 2 hours 45 minutes and the wave heights was around 58 cm.

These wave heights computed can be used to understare the kind of damage the Tsunami can cause once they reach the land. It is generally observed that when the wave arrives on land it will be 8 to 10 times greater than that of the gauge. On the east coast of India the observed run up heights were between

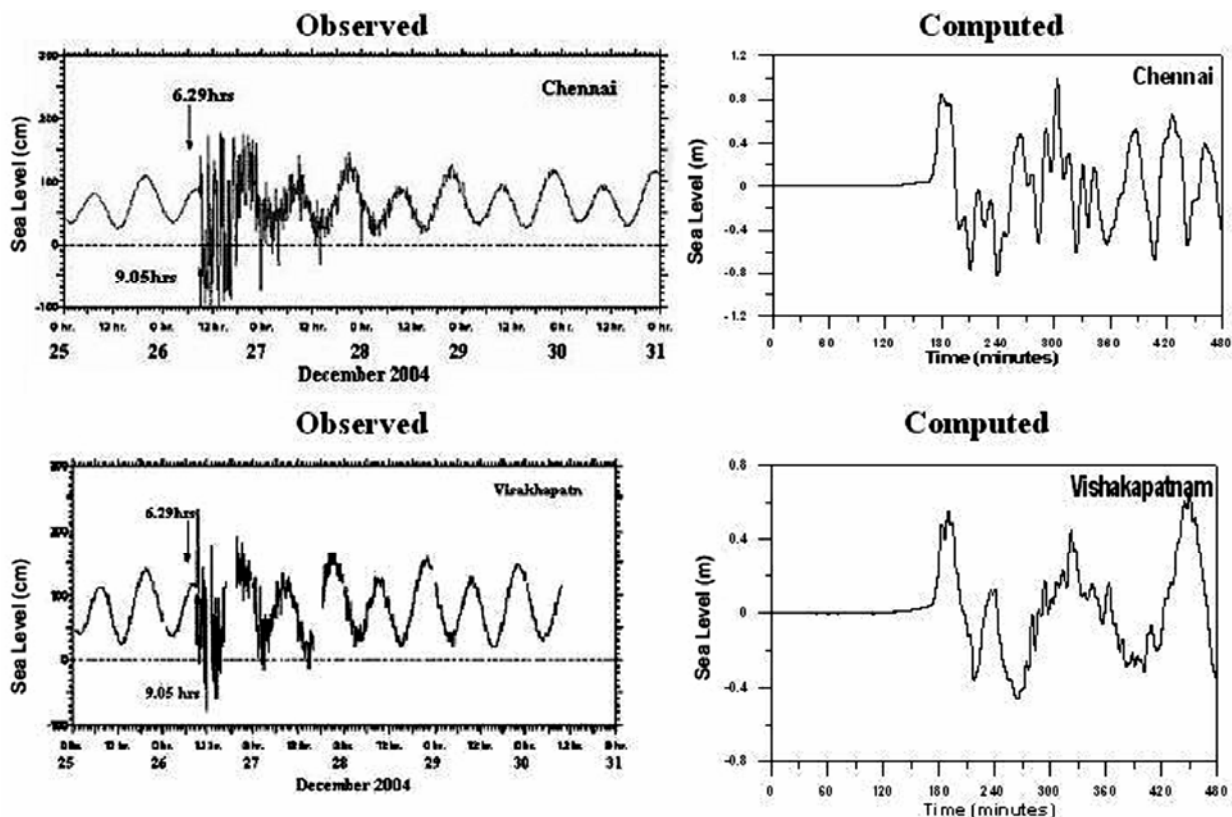


Fig. 5—Wave heights at Chennai and Visakhapatnam: observed and computed

4 to 6 m. Our modeling results seem to be in agreement with the observations of the 2004 Tsunami.

Discussion

On 26th December 2004 Indian Peninsular tsunami was triggered by an earthquake of magnitude 9.0 at 3.4° N, 95.7° E off the coast of Sumatra at 06:29 hrs IST. In order to understand the seismotectonics of this region, detailed fractal analysis of the aftershock activity has been carried out. A distinct spatial pattern is evident from the linear log-log plot i.e. the power law and is exhibited in all the zones. Linearity is seen to exist for a scale length of < 1 km in all the four zones. Comparing the b values obtained for these zones⁵ with the fractal dimension we see a correlation in all the three zones i.e zone-1, zone-2 and zone-3, i.e b is approximately equal to $2D$. However such a scenario is not evident in Zone-4. The reason for a high b value in the back arc spreading center has been attributed to a region of normal earthquakes in comparison to thrust or strike slip mechanism in the Sumatra subduction zone. This also indicates that Zones 1, 2, and 3 are thrust type earthquakes which are also observed from the focal mechanism solutions, which is a prerequisite for the generation of Tsunami. Further for any Tsunami modeling it is necessary to have reliable focal mechanisms and this can be inferred from the focal mechanism solution's and the seismotectonic studies of this region. The fractal dimension has also been obtained for all the four zones together which is around 1.9 indicating that the fault ruptures are two dimensional in nature.

The Tsunami waves traveled in the Indian Ocean and the wave propagation was controlled significantly due to reflections. They travelled and arrived in at different times at different locations on the Indian coast, for example they reached Chennai at 08.45 hrs i.e about 2 hours 16 minutes after the earthquake and Visakhapatnam around 09.05 hrs i.e about 2 hours 36 minutes. In this paper the Tsunami waves were modeled for the source parameters and the estimated time of arrival of these waves are obtained and seen to be in agreement with the observed tidal data. Also the wave heights tally with the tidal data that was observed at those locations.

Acknowledgement

Authors wish to thank Dr D. Srinagesh, Dr D.V. Ramana and Dr Simanchal Padhy for their valuable scientific discussions.

References

- 1 Ammon, C., Ji, C., Thio, H-K, Robinson, D., Ni, S., Hjorleifsdottir, V., Kanamora, H., Lay, T., Das, S., Helmberger, D., Lchinose, G., Poiet, J. & Waid, D., Rupture Process of the 2004 Sumatra – Andaman earthquake, *Science*, 308 (2005) 1133-1139.
- 2 Lay, T., Kanamora, H., Ammon, C.J., Nettles, M., Ward, S.N., Aster, R.C., Beck, S.L., Bilek, S.L., Brudzinski, M.R., Butler, R., DeShon, H.R., Ekstrom, G., Satake, K & Sipkin, S., The great Sumatra – Andaman Earthquake of 26 December, *Science*, 308, (2005) 1125-1132.
- 3 Ramasamy, S.M., & Kumanan, C.J, *Tsunami: The Indian Context*, (Allied Pub. Pvt. Ltd . Chennai, India) 2005.
- 4 Dimri, V.P. & Kirti Srivastava, Modeling techniques for understanding the Indian Ocean tsunami propagation, In *The Indian Ocean Tsunami*, edited by Tad Murthy, (Taylor & Francis, London, UK) 2006, pp. 123-130.
- 5 Ramana, D.V., Srinagesh, D & Chadha, R.K., Spatial analysis of the frequency magnitude distributions of aftershock activity of Dec 2004 Tsunamigenic Sumatra earthquake, *Curr Sci*, (2007) Communicated.
- 6 Gutenberg, B. & Richter, C., Frequency of earthquakes in California, *Bull. Seismol. Soc. Am.*, 34 (1944) 185-188
- 7 Scholz, C.H., *The mechanics of earthquakes and faulting* (Cambridge University Press, New York) 1990.
- 8 Wiemer S. & Wyss, M., Mapping the frequency – magnitude distribution in asperities: An improved technique to calculate recurrence times? *J. Geophys. Res.*, 102 (1997) 15,115-15,128
- 9 Nanjo, K., Nagahama, H., & Satomura, M., Rates of aftershock decay and the fractal structure of active fault systems, *Tectonophysics*, 287, (1998) 173-186.
- 10 Enescu B., & Ito, K., Spatial analysis of the frequency magnitude distribution and decay rate of aftershock activity of the 2000 Western Tottori earthquake, *Earth Planet Space*, 54, (2002) 847-859.
- 11 Aki, K., Maximum-likelihood estimate of b in the formula of $\log N = a - bM$ and its confidence limits, *Bull. Eathq. Res. Inst., Univ. Tokyo*, 43 (1965) 237–239.
- 12 Dimri, V.P., Vedanti, N & Sandip, C., Fractal analysis of aftershock sequence of the Bhuj earthquake: A wavelet – based approach, *Curr. Sci.*, 88 (2005) 1617-1620.
- 13 Dimri, V.P. & Srivastava, R.P., Fractal modeling of complex subsurface geological structures, In: *Fractal behavior of the earth system*, edited by V.P. Dimri (Springer, Netherlands) 2005, pp. 208.
- 14 Imamura, F., Yalciner, A.C. & Ozyurt G., *Tsunami modeling manual*, UNESCO Tsunami modeling course (UNESCO) 2006.
- 15 Imamura, F., Review of tsunami simulation with a finite difference method, long-wave runup models, edited by H. Yeh, P. Liu & C. Synolakis (World Scientific) 1996, pp. 25-42.
- 16 Yalciner A. C., Pelinovsky E., Synolakis C., & Okal E., "Submarine landslides and tsunamis", (Kluwer Academic Publishers, Netherlands) 2003, pp 329.
- 17 www.earthquakes.usgc.gov.
- 18 Wiemer S., A software package to analyze seismicity: ZMAP, *Seismol. Res. Lett.*, 72 (2001) 374-383

- 19 Catherine J.K. Gahalaut V.K. & Sahu V.K., Constraints on rupture of Dec 26, 2004 Sumatra earthquake from far field gps observations, *Earth Plan. Sci. Lett.*, 273, (2005) 673-679.
- 20 Kanamori, H., Seismological Aspects of the December 2004 Great Sumatra-Andaman earthquake, *Earthquake Spectra*, 22, (2006) pp. S1-S12
- 21 Singh S. K, Ortiz M, Gupta H. K. & Ramadass D. G. A., Slow slip below Port Blair, Andaman, during the great Sumatra-Andaman earthquake of 26 December 2004, *Geophys. Res. Lett.*, 33, (2006), L03313, doi:10.1029/2005GL025025
- 22 <http://www.nio.org/jsp/tsunami.jsp>.